Coherence resonance in a thermoacoustic system

Lipika Kabiraj,* Richard Steinert, Aditya Saurabh, and Christian Oliver Paschereit
Chair of Fluid Dynamics, Hermann-Föttinger-Institut (HFI), Technische Universität Berlin, D-10623 Berlin, Germany
(Received 22 April 2015; revised manuscript received 7 September 2015; published 6 October 2015)

We experimentally investigated the noise-induced dynamics of a prototypical thermoacoustic system undergoing a subcritical Hopf bifurcation to limit cycle oscillations. The study was performed prior to the bistable regime. Analysis of the characteristics of pressure oscillations in the combustor and fluctuations in the heat release rate from the flame—the two physical entities involved in thermoacoustic coupling—at increasing levels of noise indicated precursors to the Hopf bifurcation. These precursors were further identified to be a result of coherence resonance.

DOI: 10.1103/PhysRevE.92.042909   PACS number(s): 47.70.Pq, 05.40.−a, 43.35.Ud, 89.20.Kk

I. INTRODUCTION

Thermoacoustic instability occurs in systems such as combustors in industrial furnaces and gas turbines, where confined combustion is present. The phenomenon is a manifestation of feedback coupling [1] between acoustic oscillations in the combustor and heat release rate fluctuations from the combustion source: Acoustic fluctuations in the combustor, p', perturb the combustion source—typically single or multiple turbulent flames—leading to heat release rate fluctuations, $\dot{q}'$, which in turn add energy back into the acoustic field of the combustor by causing density fluctuations. Depending on the dimensions, distribution of temperature, hydrodynamic flow field, and boundary conditions, the combustor supports certain natural acoustic modes. Self-sustained oscillations that arise as a result of thermoacoustic coupling appear at frequencies corresponding to these acoustic modes.

The most complicated element of this feedback loop is the process of flame response to acoustic fluctuations. The flame response to acoustics is nonlinear, involves time delay, and varies primarily according to the flame type and the composition of the fuel-air mixture. It is the most important factor that governs the dynamics of thermoacoustic oscillations. With variation in a critical operating parameter, the onset of thermoacoustic instability (henceforth referred to as *instability*) occurs via a supercritical (soft) or subcritical (hard) Hopf bifurcation. In the case of a subcritical Hopf bifurcation, a bistable region exists for a range of parameter values. This region supports nonlinear phenomena such as triggering and hysteresis, which have been previously reported for thermoacoustic systems [2–5]. Most often, the state resulting from the Hopf bifurcation is a limit cycle oscillation at a frequency close to one of the acoustic resonance frequencies of the combustor. However, more complicated dynamics—quasiperiodic, chaotic, or intermittent states—can also appear at the onset, due to subsequent bifurcations of the limit cycle as reported previously in experiments [6–8] and numerical studies [9]. Transition of a combustor from steady (i.e., no coherent oscillations) operation to instability is detrimental to the system because of the resulting high-amplitude pressure oscillations and high thermal loading. For this reason, from a practical point of view, the combustor is said to be stable during steady operation and unstable when instability occurs, even though both states correspond to stable asymptotic solutions: the stable focus and one of the possible oscillatory states.

Fluctuations originating from aerodynamic noise, turbulent flames, and random modulations in the operating parameters are often a feature of practical thermoacoustic systems. Noise, therefore, is inevitably present in thermoacoustic systems. Accordingly, understanding the effect of noise on the thermoacoustic coupling is of fundamental and practical importance. However, stochastic dynamics of thermoacoustic instability has received very little attention in the community. In early studies on the effects of noise, it has been identified that, in the presence of background noise, a statistical rather than deterministic characterization of the instability is the appropriate approach because characteristics of the instability behave like random variables [10,11]. The influence of parametric noise on the stability boundaries has been investigated in Refs. [10] and [12]. The most investigated aspect, however, is the effect of noise on triggering of instabilities in the bistable region. For instance, experiments [13] and numerical studies [14] on triggering in the subcritical zone via the unstable limit cycle in the presence of varying amplitudes of noise have been carried out. It was identified that a bimodal probability distribution function of the pressure amplitudes emerges as a result of frequent transitions between the stable focus and the stable limit cycle solution in the bistable region. Noise addition facilitated this transition, and triggering could be achieved for noise amplitudes lower than the unstable limit cycle amplitude. Among the different types of noise, pink noise was found to be the most effective in triggering instability. Recently [15], the stochastic dynamics of thermoacoustic instability has also been proposed as an explanation for random transitions between deterministic modes of the instability, a phenomenon which has been observed in gas turbine combustors.

In contrast to previous studies, the focus here is on investigating the role of noise in the region of the parameter space just before the bistable region. In this region, the response of the model thermoacoustic system to external acoustic noise is studied. Experimental results that we present here show that the model thermoacoustic system studied responds to acoustic noise, even though the steady state—which corresponds to the stable focus—is the only state possible in the investigated range of parameter values. Furthermore, the system response characteristics indicate the presence of *coherence resonance* (CR) [16].

*lipika.kabiraj@tu-berlin.de

CR is the term associated with the phenomenon of noise-induced enhancement of deterministic dynamics in a nonlinear system [17]. The response of the system shows a resonance-like behavior: an optimum response results from a particular, intermediate level of noise amplitude. CR is a variant of a similar phenomenon known as stochastic resonance (SR), where the enhancement occurs in the presence of noise and an external weak deterministic signal [18,19]. SR and similar counterintuitive effects of noise have been investigated—in both experiments and numerical analyses—in a variety of nonlinear systems: physical, biological, and chemical systems, lasers, electronic circuits, and even geological studies. For a detailed review of early investigations on SR, the reader is referred to Ref. [20].

In bistable systems noise-induced CR has been shown to result in noisy precursors to the Hopf bifurcation [21–23]. The phenomenon has been previously studied in the context of stochastic dynamics of classical nonlinear oscillators [23,24]. Zakharova *et al.* [23] identified that CR in a bistable system in the "subthreshold" regime (i.e., before the bistable region) is accompanied by qualitative changes in the probability distribution: stochastic (P) bifurcations [25] of the nonlinear oscillator.

Our experiments also show that noise induces coherence in the prototypical thermoacoustic system undergoing subcritical Hopf bifurcation in the subthreshold regime. Noisy precursors [26,27] to the Hopf bifurcations, a manifestation of CR, were observed as the bistable region was approached. The bifurcation parameter that we chose is the equivalence ratio [28], ϕ. It quantifies the gaseous fuel-air mixture composition. If $\phi = 1$, the composition is such that the amount of air is exactly sufficient for the amount of fuel. For $\phi > 1$, insufficient air is present for complete combustion. ϕ determines the flame response and, hence, the dynamics of thermoacoustic coupling. Operating at $\phi < 1$ (lean combustion) is beneficial in terms of pollutant emission. However, lean combustion systems are more susceptible to thermoacoustic instability, on account of the flame being more responsive to acoustic perturbations. Thus, investigations on combustors running under lean conditions are of practical interest. We performed our experiments also under lean conditions.

The report that follows has been divided into four major sections. Section II details the main features of the experimental setup, instrumentation, and experimental methodology. Section III contains the results on the impact of noise on p' and $\dot{q}'$ fluctuations. Characterization of noise-induced coherence in the system is performed in line with previous reports on CR. Subsequently, critical observations and related inferences are discussed. In Sec. IV we state the main conclusions and implications of our report.

II. EXPERIMENTAL CONFIGURATION

Experiments were performed on a prototypical combustor (Fig. 1) consisting of an upstream plenum, a compact combustion source, and a downstream exhaust. A laminar, quasiflat, premixed, natural gas and air flame was employed as the combustion source. Flame stabilization was achieved using perforated plates: The flame stabilized immediately downstream of a copper plate of 2-mm thickness with circular holes of 2-mm diameter, arranged in a hexagonal pattern with a pitch of 4.8 mm. The diameter of the resulting flame was approximately 50 mm.

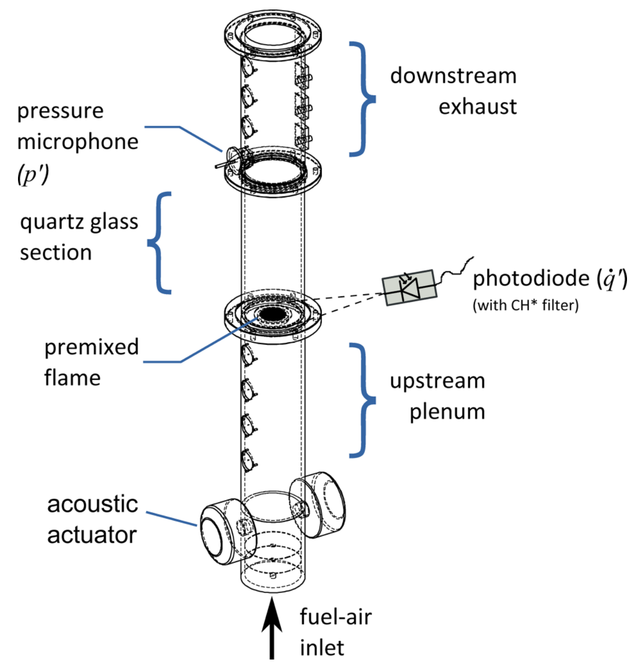

FIG. 1. (Color online) Premixed flame combustor. Noise is introduced through the acoustic actuators driven by a white-noise input voltage signal.

The flame divided the cylindrical combustor into two parts—the upstream plenum and the downstream exhaust—each with an axially uniform inner diameter of 105 mm. The 586-mm-long, stainless-steel upstream plenum was equipped with two acoustic driver (actuator) units, located 430 mm upstream of the flame, which were used as the source of acoustic noise in the experiments. The acoustic actuators were driven by Gaussian white-noise voltage signals generated via a DS1103 PPC control board at 16384 Hz. The plenum also contained the inlet for the premixed fuel-air mixture. The mixture moves vertically towards the flame after entering the plenum. The sound generated due to the mixture entering the plenum through a small inlet (4.7 mm) is a source of acoustic noise that could affect system dynamics. This noise was minimized using a muffler arrangement consisting of alternating layers of fire-resistant foam and steel disks with a 20-mm circular hole in the center, placed immediately downstream of the inlet.

The downstream exhaust duct was made of two parts of equal inner diameter. A 300-mm-long quartz glass, placed immediately downstream of the flame, formed the first part. The second part was a steel duct, 315 mm in length, with provisions to mount thermocouples for temperature measurement and water-cooled microphones for measurement of the acoustic pressure in the duct. The quartz duct allowed for the measurement of fluctuations in the chemiluminescence from CH radicals generated during combustion at the flame. Fluctuations in CH chemiluminescence from premixed flames is known to be proportional to the fluctuations in the unsteady heat release rate ($\dot{q}'$) [29].

Results presented here are based on measurements of acoustic pressure oscillations (p') in the exhaust duct using a water-cooled 1/4-in. condenser microphone, located about 350 mm from the perforated plates, and fluctuations in the luminosity of CH radicals generated at the flame, acquired using a photodiode equipped with an optical CH filter (431 nm). The water-cooled microphone setup was calibrated before the experiments. Data were acquired at a sampling rate of 8192 Hz. For each individual measurement, 32 s of data was recorded. Temperature at the interface between the downstream duct and the holder for the perforated plates was monitored using a K-type thermocouple. Experiments were performed only after the measured temperature reached a steady state. Acoustic noise introduced in the rig was varied in the range $D = 1.4$–21.2 Pa, where D is the root-mean-square (rms) of the acoustic noise level measured at the microphone location under quiescent conditions. D is interchangeably termed either the base noise level or the noise amplitude, as appropriate, in the following.

Natural gas and air flow rates were controlled and monitored using Coriolis flow meters. For the experiments, the air flow rate was fixed at 1.3 kg h^{-1} and the fuel flow rate was varied in the range from 0.052 to 0.0555 kg h^{-1}. The corresponding range of equivalence ratio $\phi = 0.688$–0.735. The standard deviation of ϕ, calculated from fuel and air flow measurements, is 0.002. In experiments, ϕ was varied in steps of 0.007. Given the dimensions of the upstream plenum, and the low values of the fuel and air flow rates, fluctuations in ϕ are expected to be lower than the measured error in ϕ, upstream of the flame. It is assumed that the mean flow velocity in the rig is governed by the air flow rate only; the variations due to fuel flow rate changes are not critical for the studies performed.

Regions in the parameter space that correspond to the stable focus (thermoacoustically stable), bistability, and stable limit cycle (thermoacoustically unstable) were identified in preliminary bifurcation experiments. These were conducted immediately before experiments on the effects of noise. In multiple realizations of the bifurcation experiment, we found that critical points did not occur consistently at the same parameter value (see also the Appendix). Here, we report the most frequently obtained critical parameter values: When increasing ϕ, the limit cycle was first obtained at $\phi = 0.728$. While decreasing ϕ, hysteresis was observed, and the system returned to the stable focus at $\phi = 0.714$. Thus, the Hopf point occurs at $\phi = 0.728$ and a subcritical zone exists between $\phi = 0.721$ and $\phi = 0.728$. This is graphically shown as the variation in the rms of p' with respect to the control parameter, ϕ, in Fig. 2. The solid and dashed curves represent the forward and reverse directions of the bifurcation analysis, respectively. The spectrum of oscillations in p' and $\dot{q}'$ during the limit cycle peaks at 191 Hz.

The bifurcation behavior and the extent of the subcritical zone (for subcritical bifurcation) are dependent on the system. For the studied configuration, the subcritical zone obtained is very small with respect to the minimum step size of parameter value variation possible, which is limited by the measurement system. The effects of noise in the subthreshold regime are expected to become weaker with the distance from the subcritical zone. Hence it was imperative to perform experiments as close to the subcritical regime as the setup configuration allows. For subsequent experiments involving noise, the chosen parameter value closest to the bistable regime corresponds to $\phi = 0.714$, where the system was found to be stable (i.e., self-excited oscillations were not present) in all the bifurcation experiments. This ensured that the experiments with noise were conducted in the subthreshold regime. In addition to the bifurcation experiments, triggering tests were conducted. Triggering was not observed at the said parameter value, $\phi = 0.714$.

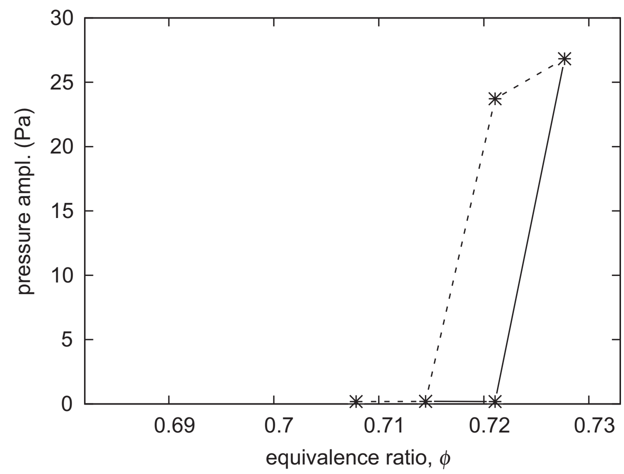

FIG. 2. Subcritical Hopf bifurcations in the noise-free thermoacoustic system. The acoustic pressure amplitude, rms[p'], as a function of the control parameter, ϕ. The solid line connects experimental points obtained while increasing ϕ, while the dashed line indicates translation in the reverse direction.

III. RESULTS

We conducted experiments for equivalence ratios prior to $\phi = 0.721$ (see Fig. 2). The response of the system at each ϕ to increasing levels of noise was recorded in terms of p' and $\dot{q}'$ fluctuations. Exemplary results reported here correspond to noise amplitudes $D = 5.7$, 9.9, and 14.2 Pa, unless specified otherwise.

At first, the rms amplitudes of p' and $\dot{q}'$ fluctuations were analyzed (Figs. 3 and 4). The curves correspond to the system response to different noise levels, as indicated in the figures. The base noise levels (dashed lines) are included for p' fluctuations (Fig. 3) for comparison. The shaded region marks the bistable and thermoacoustically unstable (stable limit cycle) regime. The forward direction of the bifurcation analysis is included for comparison (rightmost curve, with asterisks). At a low noise level ($D = 5.7$ Pa), p' fluctuations were found to coincide with the base noise level till the edge of the bistable zone. However, as the noise level was increased, p' rms curves deviate from the base noise level towards higher amplitudes. The system response to noise increased as it was brought closer to the bistable region: $\phi = 0.714$ had the most prominent response. These observations can be regarded as indications of a nontrivial system response to noise in the subthreshold region. The observation that the system response is higher than the base noise level when the flame is present indicates that the p'-$\dot{q}'$ coupling process is affected

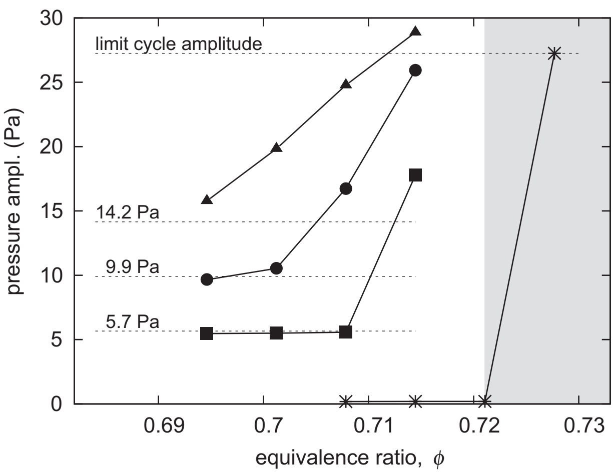

FIG. 3. Amplitude of p' fluctuations in response to varying levels of noise in the subthreshold region: $D = 5.7$ Pa (squares), $D = 9.9$ Pa (circles), and $D = 14.2$ (triangles). The shaded region indicates the bistable and the thermoacoustically unstable zones. Base noise levels (horizontal dotted lines) and the forward direction of bifurcation analysis (asterisks) are included for reference.

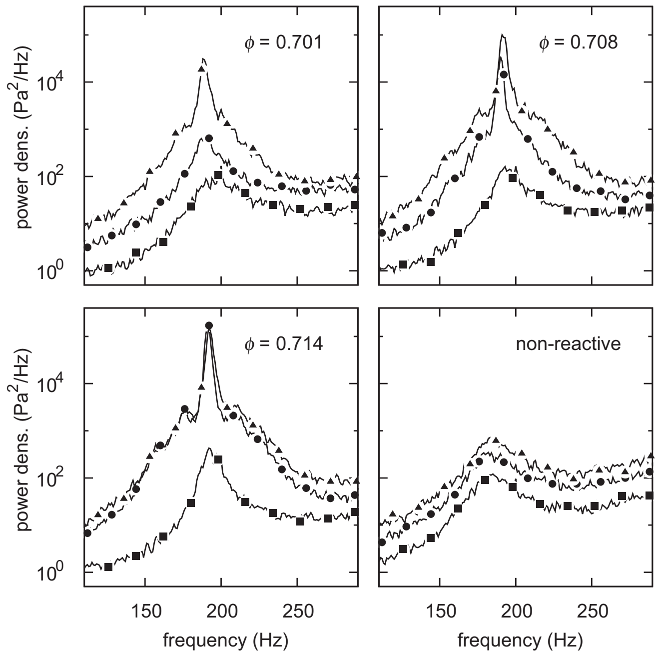

FIG. 5. Power spectra from p' for different equivalence ratios and nonreacting flow (bottom-right). Curves correspond to the three noise levels: $D = 5.7$ Pa (squares), $D = 9.9$ Pa (circles), and $D = 14.2$ Pa (triangles).

by the external noise. Also supporting this argument is the observation that the rms curves for $\dot{q}'$ (Fig. 4) follow a trend identical to that observed for p' fluctuations.

Further details on the system response to noise were observed in the spectral decomposition of the fluctuations. Figure 5 shows the frequency spectra of p' fluctuations for different values of ϕ. The three curves in each frame correspond to the three levels of noise amplitude. The nonreacting case (bottom-right) has been included for comparison. In the nonreacting case, noise addition resulted in a uniform increase in the power across all frequencies. The bump around 180 Hz corresponds to the acoustic mode of the duct, which also participates in p'-$\dot{q}'$ coupling during self-excited oscillations.

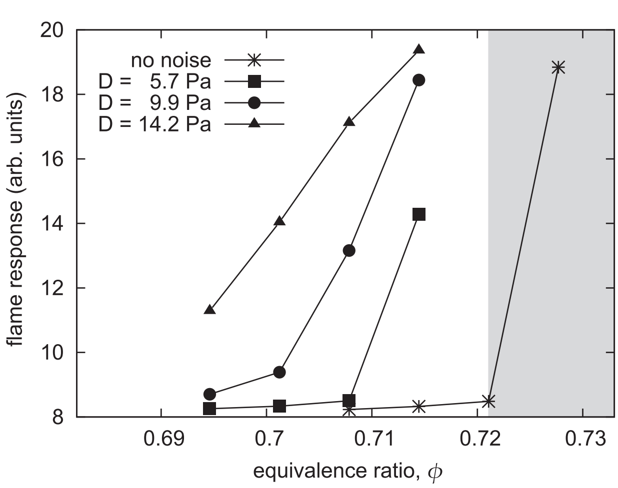

FIG. 4. Amplitude of $\dot{q}'$ fluctuations in response to varying levels of noise in the subthreshold region: $D = 5.7$ Pa (squares), $D = 9.9$ Pa (circles), and $D = 14.2$ (triangles). The shaded region indicates the bistable and the thermoacoustically unstable zones. The forward direction of bifurcation analysis (asterisks) is included for reference.

Under reacting conditions, a pronounced response at 191 Hz was observed in the presence of noise. The shift in the peak frequency compared to the nonreacting state is due to the increased temperature in the presence of the flame. A rise in the spectral peak with increasing noise levels can be seen for the three reacting cases. At the same level of noise, the spectral peak becomes more distinct as ϕ increases (i.e., as the system is brought closer to the bistable region). For instance, at $\phi = 0.708$, in response to the noise level at 9.9 Pa, the spectral peak can be seen to be higher compared to the peak at $\phi = 0.701$. As an additional observation, a slight shift of the peak towards lower frequencies with increasing noise amplitude was observed for the reacting cases.

Noise-induced changes in the spectral peaks were further quantified on the basis of the coherence factor, β [16,22,23,27]. β is defined as the ratio between the spectral height (H) and the normalized spectral width (normalized by the peak frequency): $\beta = H * (\Delta f / f_p)^{-1}$. Here, Δf is the full width at half-maximum of a Lorentzian (least-squares) fit to the spectra around the peak frequency. In the presence of nonlinearity, both the peak height and the width are affected by noise [30]. If CR is responsible for the system response to noise in the subthreshold region, the combined effect of noise on the spectral peak is such that β passes through a maximum for intermediate noise levels [27].

The β curves for the cases under discussion are shown in Fig. 6. The curves were obtained from the spectra of p' fluctuations. Each point is the mean of data obtained from seven experiments. For $\phi = 0.714$, which is the closest point in the investigation to the bistable region, β has a clear maximum at $D = 12.7$ Pa. The same trend is found for $\phi = 0.708$ and 0.701, which are farther away from the bistable region: β

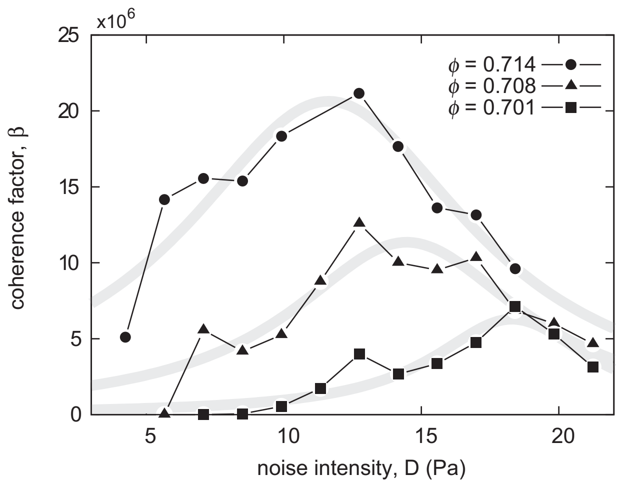

FIG. 6. Coherence factor, β, as a function of the noise level for different equivalence ratios. A maximum occurs for an optimum noise level for each curve, indicating coherence resonance. As exemplified by the Lorentzian fits (gray bands), the optimum value decreases with an increase in ϕ.

initially increases with D and subsequently decreases. Maxima can be identified close to $D = 12.7$ Pa for $\phi = 0.708$ and about $D = 18.4$ Pa for $\phi = 0.701$, although they are not as pronounced as for $\phi = 0.714$. As is expected from CR [27], a shift of the noise amplitude that induces maximum coherence to higher values with an increase in the separation from the bistable region can be inferred from the plot. This behavior is exemplified by the Lorentzian fits to the data points and is shown in the plot as gray bands. Identical trends in the coherence factor were also obtained for $\dot{q}'$ fluctuations.

Noise-induced coherence can further be examined through the autocorrelation of the fluctuations [17,23]. In Fig. 7, the temporal autocorrelation of p' for different levels of noise is shown. A visual comparison clearly shows that at

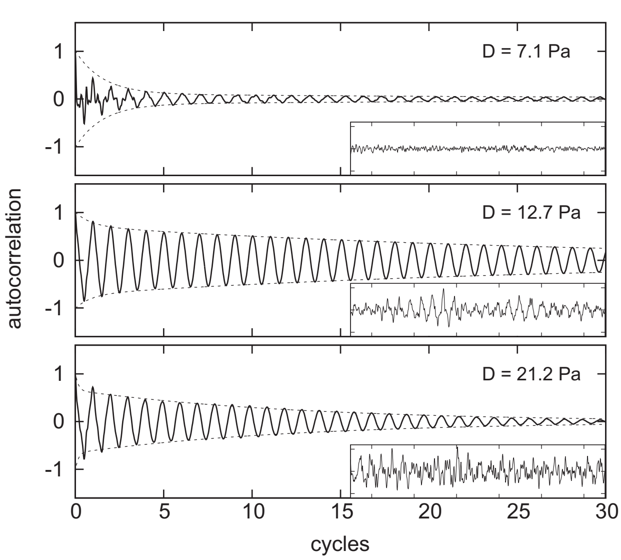

FIG. 7. Autocorrelation from p' for $\phi = 0.708$ at three noise levels. Decay in the autocorrelation is the slowest for $D = 12.7$ Pa. Insets: Sections from the corresponding time series.

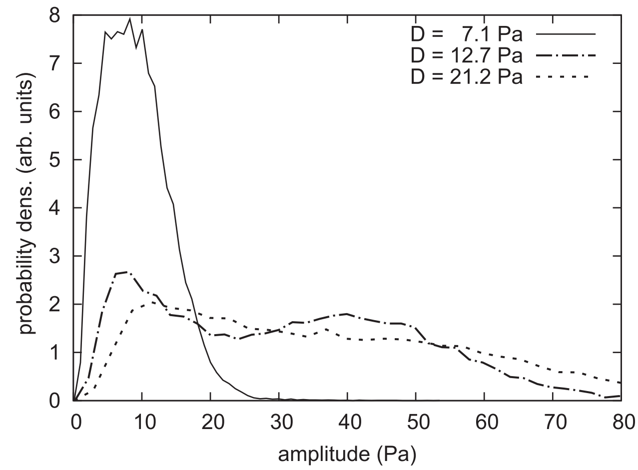

FIG. 8. Amplitude distribution for p' at three noise levels. The distribution changes from a unimodal to a bimodal and back to a unimodal distribution with increasing noise intensity.

the intermediate noise level, $D = 12.7$ Pa, the decay in the autocorrelation of the time series is slower than at lower ($D = 7.1$ Pa) or higher ($D = 21.2$ Pa) noise amplitudes. Thus, in the subthreshold region, there exists an optimum level of noise that induces the most coherence in the system. Decreasing as well as increasing the noise intensity results in a relatively lower amplification of coherent fluctuations. In the corresponding time series, shown as insets in Fig. 7, coherent oscillations appear for short time intervals within the noisy pressure time series. The appearance is most pronounced for the intermediate level of noise, $D = 12.7$ Pa. At $D = 21.2$, coherent oscillations superimposed with noise can be observed. The difference between the cases is clearly captured by the corresponding autocorrelation curves.

In Ref. [23], it has been illustrated that the coherence-like response of the system to noise in the stable regime is associated with stochastic P bifurcations, which can be identified as qualitative changes in the amplitude distribution of the fluctuations with increasing noise levels. Results of our experiments also correspond to this explanation. The amplitude distributions calculated from noise-induced p' fluctuations are presented in Fig. 8. At a low noise level, the amplitude distribution is unimodal in shape, with a peak close to the noise level. As the noise level is increased, the shape of the distribution changes, and at $D = 12.7$ Pa, it assumes a bimodal shape, with the second peak close to the expected amplitude of the limit cycle (∼40 Pa). Further increase in the noise level results in another unimodal distribution that peaks at an amplitude close to—albeit higher than—the lower of the two peak amplitudes of the previous bimodal distribution.

IV. DISCUSSION

This experimental study of the thermoacoustic system was motivated by the observations of noise-induced order that is manifested as noisy precursors, stochastic bifurcations, SR, and CR in several bistable and excitable systems. Studying the effects of noise on model thermoacoustic systems, we find that the introduction of noise does induce coherent dynamics in the system prior to the subcritical Hopf bifurcation.

The induced coherence was reflected in the characterization of the spectral peak and the temporal autocorrelation of p' and $\dot{q}'$ fluctuations. The spectral peak that emerged due to the addition of noise appeared at the frequency of the stable limit cycle associated with the subcritical Hopf bifurcation. This result corresponds to observations made previously on an electrochemical system undergoing a supercritical Hopf bifurcation [22]. Variations in the spectral peak characteristics also correspond to results on the effects of noise that have been reported previously for other nonlinear systems [23,24]. Quantifying the changes in the spectral peak through the coherence factor, β, a resonance-like response, where an optimum is obtained at an intermediate noise level, was identified. In line with previous studies on CR in nonlinear systems [16,22,23], this result clearly indicates the presence of CR in the investigated thermoacoustic system. Furthermore, we also could identify the occurrence of stochastic *P* bifurcations together with CR, as discussed in Ref. [23].

For thermoacoustic instability, which can be described by a set of delay differential equations representing the time-delayed feedback coupling between p' and $\dot{q}'$ [31], stochastic limit cycles are created by noise. This coherence-inducing effect is related to the proximity of the system to the bistable region. This inference is derived from the observation that the optimum amplitude of noise is a function of the bifurcation parameter: it decreases with increasing proximity to the bistable region. In addition, the frequency of the stochastic limit cycles corresponds to the frequency of the nearby stable limit cycle state. Competition between induced coherent and incoherent fluctuations—both of which are due to introduced noise—results in a resonance-like behavior [27], where the optimum system response occurs at intermediate levels of noise. In addition, while in this work we have considered the case of subcritical Hopf bifurcation, based on the result in Ref. [22], CR can be expected to be present in thermoacoustic configurations that undergo transition to limit cycle oscillations via supercritical Hopf bifurcation.

It should be noted that although the input signal to the acoustic actuators—the noise sources—was Gaussian white noise, the noise that actually participates in the p'-$\dot{q}'$ coupling process might be colored. This is because the combined acoustic properties of the actuator and the combustor will modify the input noise signal. However, it has been shown previously that noise-induced coherence also exists in the presence of colored noise [32].

As mentioned before, investigations of the effect of noise in thermoacoustic systems have been restricted to the bistable region. However, observations of random and isolated (intermittent) occurrences of periodic bursts prior to the occurrence of instability have been made previously in model thermoacoustic systems [2,33]. Here, we show that if noise is introduced below the saddle node of the bistable region, oscillatory behavior is induced in the system. In light of the results presented here, it is possible that these previous observations of intermittent coherent dynamics are associated with CR, which was induced by inherent noise due to flow turbulence and combustion noise.

These findings are a critical result in the stochastic dynamics of thermoacoustic systems. As practical applications of these results, it might be possible to incorporate this new understanding of noise-induced coherence in thermoacoustic systems as a precursor that indicates an approaching instability. Our experimental findings also support the generalization of CR as a feature of time-delayed systems undergoing Hopf bifurcations. The present study should also motivate modeling the stochastic dynamics of a naturally occurring nonlinear phenomenon that is also of interest for practical systems.

V. CONCLUSIONS

Through systematic experiments we have obtained experimental confirmation of noise-induced coherence in a thermoacoustic system undergoing subcritical Hopf bifurcation, in the subthreshold region—the region prior to the bistable region. We found noisy precursors to the approaching bifurcation. The response of the system to noise was characterized on the basis of temporal and spectral features of the pressure and heat release rate fluctuations. An intermediate level of noise amplitude resulted in an optimum system response. The noise level required for this optimum response decreases as the system is brought closer to the bistable region. These observations correspond to CR. CR in our system is also found to be associated with the previously proposed stochastic *P* bifurcations, where the noise level is a bifurcation parameter. This experimental report shows that noise-induced coherent dynamics, which has been reported for a variety of nonlinear bistable and excitable nonlinear systems, is also present in the time-delayed feedback coupling phenomenon known as thermoacoustic instability.

ACKNOWLEDGMENTS

We gratefully acknowledge Barbara Gentz and Anna Zakharova for insightful discussions. We are thankful also to the anonymous reviewers for their critical comments. Lipika Kabiraj would like to acknowledge the financial support (Grant

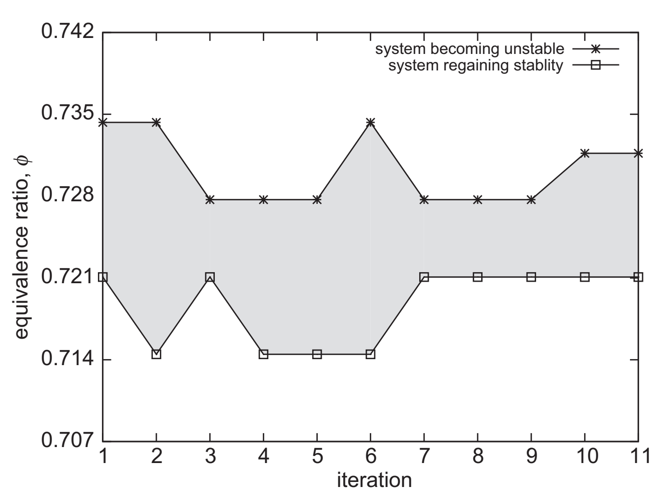

FIG. 9. Iterations of the bifurcation experiments and the obtained critical parameter values. The shaded region marks the hysteresis zone for each iteration.

No. KA 3968/1-1) awarded by the DFG (German Research Foundation) to carry out research at the Technische Universität Berlin.

APPENDIX

In bifurcation experiments, we observed that the hysteresis (or the bistable) zone associated with the subcritical bifurcation undergoes slight shifts from one experiment to another. This is shown in Fig. 9. The plot contains results of 11 bifurcation experiments. The points were obtained by increasing the parameter, ϕ, until the appearance of self-excited oscillations (asterisks) and subsequently reducing ϕ until the oscillations disappeared (squares). In the last two measurement iterations, ϕ was varied in smaller steps (0.0035). However, on the grounds of being too close to the error in ϕ measurements (0.002), experiments with noise were conducted with a step size of 0.007. It can be noted that at $\phi = 0.714$, which is the maximum equivalence ratio at which experiments to detect the presence of CR were conducted, the system state corresponds to a stable focus in all the experiments.

[1] J. W. S. Rayleigh, Nature **18**, 319 (1878).
[2] T. C. Lieuwen, J. Propul. Power **18**, 61 (2002).
[3] N. Noiray, D. Durox, T. Schuller, and S. Candel, J. Fluid Mech. **615**, 139 (2008).
[4] M. P. Juniper, J. Fluid Mech. **667**, 272 (2010).
[5] L. Kabiraj and R. I. Sujith, ASME Turbo Expo, GT2011-46155 (2011).
[6] H. Gotoda, T. Miyano, and I. G. Shepherd, Phys. Rev. E **81**, 026211 (2010).
[7] H. Gotoda, H. Nikimoto, T. Miyano, and S. Tachibana, Chaos **21**, 013124 (2011).
[8] L. Kabiraj, A. Saurabh, P. Wahi, and R. I. Sujith, Chaos **22**, 023129 (2012); L. Kabiraj and R. I. Sujith, J. Fluid Mech. **713**, 376 (2012); L. Kabiraj, A. Saurabh, N. Karimi, A. Sailor, E. Mastorakos, A. P. Dowling, and C. O. Paschereit, Chaos **25**, 023101 (2015).
[9] K. Kashinath, I. C. Waugh, and M. P. Juniper, J. Fluid Mech. **761**, 399 (2014).
[10] P. Clavin, J. S. Kim, and F. A. Williams, Combust. Sci. Technol. **96**, 61 (1994).
[11] F. E. C. Culick, L. Paparizos, J. Sterling, and V. Burnley, in *Proceedings of the AGARD Conference on Combat Aircraft Noise* (Advisory Group for Aerospace Research and Development, North Atlantic Treaty Organization, Neuilly sur Seine, France, 1992), p. 512; V. S. Burnley and F. E. C. Culick, Int. J. Energetic Mater. Chem. Propul. **4**, 998 (1997); AIAA J. **38**, 1403 (2000).
[12] T. Lieuwen and A. Banaszuk, J. Propul. Power **21**, 25 (2005).
[13] V. Jegadeesan and R. Sujith, Proc. Combust. Inst. **34**, 3175 (2013).
[14] I. Waugh and M. P. Juniper, Int. J. Spray Combust. Dynam. **3**, 225 (2011); I. Waugh, M. Geuß, and M. Juniper, Proc. Combust. Inst. **33**, 2945 (2011).
[15] N. Noiray and B. Schuermans, Proc. R. Soc. London A **469**, 20120535 (2012).
[16] G. Hu, T. Ditzinger, C. Z. Ning, and H. Haken, Phys. Rev. Lett. **71**, 807 (1993); T. Ditzinger, C. Z. Ning, and G. Hu, Phys. Rev. E **50**, 3508 (1994).
[17] A. S. Pikovsky and J. Kurths, Phys. Rev. Lett. **78**, 775 (1997).
[18] F. Moss, D. Pierson, and D. O'Gorman, Int. J. Bifurcat. Chaos **04**, 1383 (1994).
[19] R. Benzi, A. Sutera, and A. Vulpiani, J. Phys. A **14**, L453 (1981).
[20] L. Gammaitoni, P. Hänggi, P. Jung, and F. Marchesoni, Rev. Mod. Phys. **70**, 223 (1998).
[21] S. Katsev and I. L'Heureux, Phys. Rev. E **61**, 4972 (2000).
[22] I. Z. Kiss, J. L. Hudson, G. J. E. Santos, and P. Parmananda, Phys. Rev. E **67**, 035201(R) (2003).
[23] A. Zakharova, T. Vadivasova, V. Anishchenko, A. Koseska, and J. Kurths, Phys. Rev. E **81**, 011106 (2010); A. Zakharova, A. Feoktistov, T. Vadivasova, and E. Schöll, Eur. Phys. J. Spec. Topics **222**, 2481 (2013).
[24] O. V. Ushakov, H.-J. Wünsche, F. Henneberger, I. A. Khovanov, L. Schimansky-Geier, and M. A. Zaks, Phys. Rev. Lett. **95**, 123903 (2005).
[25] L. Arnold, *Random Dynamical Systems* (Springer, Berlin, 1998).
[26] K. Wiesenfeld, J. Stat. Phys. **38**, 1071 (1985).
[27] A. Neiman, P. I. Saparin, and L. Stone, Phys. Rev. E **56**, 270 (1997).
[28] The equivalence ratio, ϕ, quantifies the fuel-air ratio used with regard to the stoichiometric fuel-air ratio that is specific to the particular fuel.
[29] Y. Hardalupas and M. Orain, Combust. Flame **139**, 188 (2004).
[30] R. Stratonovich, *Topics in the Theory of Random Noise*, Vol. 2 (CRC Press, Boca Raton, FL, 1967).
[31] P. Subramanian, R. I. Sujith, and P. Wahi, J. Fluid Mech. **715**, 210 (2013).
[32] Y. Xu, R. Gu, H. Zhang, W. Xu, and J. Duan, Phys. Rev. E **83**, 056215 (2011).
[33] V. Nair and R. I. Sujith, J. Fluid Mech. **747**, 635 (2014).